Microclimatic buffering in forests of the future: The role of local water balance

Kimberley Davis[1,2], Solomon Z. Dobrowski[2], Zachary A. Holden[3], Philip E. Higuera[1], John T. Abatzoglou[4]

[1]Department of Ecosystem and Conservation Sciences, University of Montana, 32 Campus Dr., Missoula, MT, 59812

[2]Department of Forest Management, University of Montana, 32 Campus Dr., Missoula, MT, 59812

[3]U.S. Forest Service Region 1, Building 26 Ft. Missoula, Missoula, MT, 59807

[4]Department of Geography, University of Idaho, 875 Perimeter Dr, Moscow, ID, 83844

Corresponding author: Kimberley Davis, Department of Ecosystem and Conservation Sciences, University of Montana, 32 Campus Dr., Missoula, MT, 59812. Email: kimberley.davis@umontana.edu

Decision date: 07-Jun-2018

Abstract

Forest canopies buffer climate extremes and promote microclimates that may function as refugia for understory species under changing climate. However, the biophysical conditions that promote and maintain microclimatic buffering and its stability through time are largely unresolved. We posited that forest microclimatic buffering is sensitive to local water balance and canopy cover, and we measured this effect during the growing season across a climate gradient in forests of the northwestern United States (US). We found that forest canopies buffer extremes of maximum temperature and vapor pressure deficit (VPD), with biologically meaningful effect sizes. For example, during the growing season, maximum temperature and VPD under at least 50% forest canopy were 5.3°C and 1.1 kPa lower on average, respectively, compared to areas without canopy cover. Canopy buffering of temperature and vapor pressure deficit was greater at higher levels of canopy cover, and varied with water balance, implying that buffering effects are subject to changes in local hydrology. We project changes in the water balance for the mid-21st century and predict how such changes may impact the ability of western US forests to buffer climate extremes. Our results suggest that some forests will lose their capacity to buffer climate extremes as sites become increasingly water limited. Changes in water balance combined with accelerating canopy losses due to increases in the frequency and severity of disturbance will create potentially non-linear changes in the microclimate conditions of western US forests.

Keywords: climate extreme, forest, microclimate, microclimate buffering, microrefugia, water balance

Introduction

Forests are the dominant terrestrial ecosystem on the planet comprising 80% of all plant biomass and harboring the majority of species on Earth (Pan et al. 2013). This biodiversity is due in part to the diversity of microclimates created by trees (Ricklefs 1977, Hietz and Briones 1998, Chen et al. 1999, Gehlhausen et al. 2000, Cardelús and Chazdon 2005, Grimbacher et al. 2006). While forest microclimates have long been studied (Chen et al. 1999, Geiger et al. 2003), the implications of microclimates for understanding climate change impacts on biota is increasingly garnering attention, particularly given concerns about rapid warming and deforestation driven by anthropogenic and natural causes.

It is well known that trees serve to buffer understory environments from climate extremes (Chen et al. 1999, Suggitt et al. 2011, von Arx et al. 2013, Frey et al. 2016). This buffering may promote microclimates that function as microrefugia, locations that provide favorable local climate conditions amidst unfavorable regional conditions (Dobrowski 2011, Keppel et al. 2012, Hylander et al. 2015, McLaughlin et al. 2017). For example, understory plant communities in dense temperate forests showed less evidence of compositional shifts towards warm adapted taxa than sites with lower canopy cover (De Frenne et al. 2013). This was presumed to be due to the moderating effect of forest canopies on regional warming. Further, it has been suggested that forest canopies, in combination with topography, can create conditions that are decoupled from regional warming (Lenoir et al. 2017). However, if and how the buffering capacity of forests may vary through time is poorly understood, as most studies are descriptive and based on short term (1-3 year) collections of meteorological data (Breshears et al. 1998, Suggitt et al. 2011, Ashcroft and Gollan 2013, Frey et al. 2016, Kovacs et al. 2017). If microclimatic buffering is ephemeral, then refugia created by forest canopies will be transient, particularly at sites becoming warmer and drier (Hannah et al. 2015, McLaughlin et al. 2017).

The magnitude of canopy buffering effects, their stability in a changing climate, and the implications of microclimatic buffering for understanding climate change impacts on biota are largely unresolved. Research in this area uses the terms ‘buffering’ and ‘decoupling’ loosely, further adding to confusion on the topic. We view these as separate but related phenomenon (Lenoir et al. 2017). Forest microclimatic buffering is the moderation of extreme conditions in the understory (e.g. daily temperature or vapor pressure deficit). However, microclimates in buffered areas may still track regional climate trends. In contrast, decoupling occurs when a microclimate at a site is effectively isolated from macroclimatic conditions, for example within talus slopes

(Varner and Dearing 2014). Under these conditions, local climate dynamics are driven by processes that are largely independent of regional influences, although there is ambiguity about how strong this effect must be and how long a site must be isolated from regional conditions to be considered "decoupled" (Varner and Dearing 2014, Locosselli et al. 2016, Lenoir et al. 2017).

Forest microclimatic buffering is due largely to interception and attenuation of incident shortwave radiation and conversion of this energy to latent as opposed to sensible heat flux, which requires evapotranspiration in order to occur. Consequently, we examine these processes through the lens of the local water balance which describes the concomitant availability of energy and useable water for plants (Stephenson 1990). A water-balance framework is useful for assessing microclimatic buffering because the interaction of energy and water and their timing (i.e. actual evapotranspiration and unmet atmospheric demand for water – climatic water deficit) drives the ratio of latent to sensible heat flux and in turn, should influence the amount of microclimatic buffering at a site. Indeed, evidence suggests that microclimatic buffering varies by regional hydrological conditions (Ashcroft and Gollan 2013, von Arx et al. 2013, Holden et al. 2016). Therefore, understanding the relationship between water balance and microclimatic buffering in forests may improve our understanding of the stability of microclimates through time. Here we ask: How will climate change affect the ability of forests to buffer climate extremes? Specifically, (1) to what extent do forest canopies buffer temperature and vapor pressure deficit extremes during the growing season? 2) How does this buffering effect vary with local water balance? and 3) What are the implications of this for the ability of forests to buffer climate extremes in the future?

Materials and methods

Field Methods

We measured microclimatic buffering of forest canopies at three locations across a climate gradient in the northwestern U.S. (Fig. 1): the Oregon State University Dunn Experimental Forest, Oregon; the Clearwater National Forest in northern Idaho; and the University of Montana Lubrecht Experimental Forest in Greenough, Montana. At each location we established two sites, one at low and one at high elevation, for a total of six sites (Table 1).

Sites were centered on a forest clearing at least 100 m in diameter, which served as a reference for no canopy cover. Surrounding each clearing, six subplots were opportunistically placed in a way that captured a range of canopy covers, maintained similar slope and aspect, and maintained a minimum distance from the control site (~100 m) in order to minimize edge effects. At one site, Lubrecht-high elevation, logistical problems resulted in a total of five subplots. At each subplot, LogTag temperature and relative humidity sensors (accurate to 0.1 °C and 0.1% RH; model HAXO-8, LogTag Recorders, Auckland, New Zealand) were attached to a PVC pole at 2 m ('high') and 10 cm ('low') above the ground, within radiation shields that perform similarly to commercially available non-aspirated Gill shields in open and forested conditions (Holden et al. 2013). The sensors recorded temperature and relative humidity every 30 minutes. Canopy cover at each subplot was measured at two scales. First, at the 'stand' scale, a densitometer was used to note presence of canopy at five points in each cardinal direction from the sensor post with 2 m between each measurement (total 20 points). Percent canopy cover was derived from the number of points with canopy divided by the total number of points measured. Second, at the point of the sensor post, canopy cover was measured with an upward facing photograph and the 'CanopyApp'. Measurements with this app were compared to point measurements from a spherical densiometer (Fig. S2) and the two were strongly correlated (R^2=0.87). Canopy cover was also highly correlated between the point and stand scales (R^2=0.84; Fig. S1). Point measurements were used for further analysis. Sensors were deployed over three years: from August through October in 2014 and following snowmelt (May-June) through October in 2015 and 2016. Analysis was conducted for dates that included data from all sites.

Analysis

All climate data were both visually and quantitatively checked for potential errors. Mean temperature values within a site were calculated for each hour of each day, and observations from individual sensors within each site that were greater than three standard deviations from the overall site mean were visually inspected for potential sensor failures. In total, 2.8% of the data from high sensors and 0% of data from low sensors were removed from the analysis.

Vapor pressure deficit was calculated for each sensor at each time step (30 minutes) as the difference between saturated (P_{sat}) and effective water pressure of the air (P_{air}) with the following equations, where T is

temperature (in degrees Celsius) and *RH* is relative humidity (c.f. Monteith and Unsworth 2008, von Arx et al. 2013):

$$P_{\text{sat}} = 0.6112 \times \exp(((17.62 \times T))/(T + 243.12))$$

$$P_{\text{air}} = P_{\text{sat}} \times RH/100$$

Data were then aggregated to daily maximum and minimum temperatures, maximum vapor pressure deficit, and minimum relative humidity. For each subplot with varying canopy cover, we calculated daily buffering (delta maximum temperature (ΔMXT); delta minimum temperature (ΔMNT); delta maximum VPD (ΔVPD)) by subtracting the values at each sensor from the reference sensor post with no canopy cover; we did this for each day at each site and for each sensor post height (i.e. low and high). We also calculated the difference between the low sensors in the forest and the high sensor in the open (delta low-to-high maximum temperature (ΔMXT.LH); delta low-to-high minimum temperature (ΔMNT.LH); delta low-to-high VPD (ΔVPD.LH)), to help quantify the differences between standard climate products (derived from weather stations 2 m above the ground) and microclimate conditions that understory plants experience.

We modeled solar radiation, average wind speed, and soil moisture for each subplot to use as predictors of daily ΔMXT, ΔMNT, and ΔVPD. Daily total solar radiation, and air temperature data were extracted at each subplot from 8 arc-second (~ 250 meter) resolution grids described by Holden et al. (2016) and extended to cover the northwestern US study domain. Wind speed data at each site was retrieved from the Real-Time Mesoscale Analysis (RTMA; De Pondeca et al. 2011). To approximate the wind speed at the time of maximum daytime temperature, we used the value from 2200Z (3 pm local time). The RTMA blends weather model data with surface observations from stations sited almost exclusively in locations with no canopy cover. Our modeled values are not meant to reflect the actual wind speed values at the ground level at each subplot but are instead meant to capture site level differences associated with landscape position and exposure to dominant wind directions. They represent an index of windiness for each day. These data were used with daily 4-km resolution precipitation data described by Abatzoglou (2013) to run a simple soil water-balance model adapted from Dobrowski et al. (2013) to run at daily time steps. To better estimate near-surface soil moisture and its effect on

sensible heating, soil water holding capacity was fixed at 100 mm, such that any precipitation exceeding that capacity was assumed to be runoff or lost to deeper soil layers.

Daily microclimatic differences

To assess daily differences in temperature and VPD between the forests and clearings during the growing season, we modeled ΔMXT, ΔMNT, and ΔVPD with linear mixed effects models as a function of percent canopy cover, soil moisture, solar radiation, average wind speed, and minimum daily RH (temperature responses only). These predictors vary at the daily time step and contribute to the local water balance of the subplot. The data from the high and low sensors were modeled separately. Second order polynomial terms for each explanatory variable and up to three-way interactions were included in candidate models to maximize our ability to represent patterns in the response. Random intercept terms for the effects of subplot nested within site were included in all models to account for repeated measurements from the same sensors. The final model for each response was selected based on root mean squared error (RMSE) from a spatially independent six-fold cross validation whereby data from one site was left out and used for validation, data from the remaining five sites was used for calibration, and the process was repeated for each site. We chose this conservative approach of selecting models to ensure that our final models would not be overfit and would be transferable. The residuals of the best models for each response variable were examined for serial autocorrelation with a correlogram. To select an optimal model while minimizing serial autocorrelation, we employed a temporally lagged 5-fold cross validation procedure. We found that the average lag period for significant autocorrelation was three days; thus, to minimize potential effects of serial autocorrelation, we subsampled each time series at a 5-day time step (one daily value was retained for each five-day time period resulting in 1178 daily observations). We then fit and assessed model skill of candidate models, and repeated this procedure a total of five times, averaging RMSE across the five folds. If candidate models had average RMSE values within 0.01 °C or 0.01 kPa of each other, the top model was chosen based on lowest Bayesian information criterion value.

Buffering Capacity

To summarize the microclimatic buffering effect of forest canopies across a range of biophysical conditions, we fit a linear model between daily measurements of maximum temperature or VPD for each

understory sensor and the same measurement made at reference sensors at the same height during each growing season (Fig. 2). The slope of this line serves as a measure of microclimate variability and has been described as a measure of "decoupling" when the reference sensor represents free air conditions (Lenoir et al. 2017 and citations therein). We initially explored the relationship between this slope and biophysical factors, but we found that sites with similar slopes can actually have substantially different amounts of microclimatic buffering across different conditions (Fig. 2). Therefore, we developed a novel metric of buffering capacity based on the summed area between the fitted and 1:1 line which discerns between conditions in which understory sites are warmer/drier or cooler/wetter than reference sites (Fig. 2). This metric captures the combined effect of the decoupling and buffering processes. We refer to this summed area as a "buffering capacity" (BC) metric, where negative BC values indicate cooler and/or moister conditions in the forest compared to the reference site and positive BC values indicate the opposite.

To examine how buffering capacity varies spatially across biophysical gradients we calculated the average growing season BC over the three growing seasons at each sensor, which we posited would covary with the water balance and canopy cover of the site. We modeled this 3-yr average buffering metric for each sensor (n=35) as a function of canopy cover and the average AET-to-deficit ratio (AET/climatic water deficit) with linear mixed effects models. AET-to-deficit ratio was calculated over the study period (2014-2016) at each subplot with 800-m monthly climate data from PRISM (Daly et al. 2008) with supplemental radiation and winds bilinearly interpolated from Abatzoglou (2013). We used a monthly (rather than a daily) water balance model to allow for predictions across broader spatial scales and to improve compatibility with future climate datasets. We tested for non-linear relationships with generalized additive models, but all patterns were linear. We included site as a random effect in all models, and degrees of freedom were estimated with Kenward-Roger approximations (Kuznetsova et al. 2014). Sensors at different heights were modeled separately.

Extrapolating to northwestern U.S. forests

Using the models described above, we predicted BC for maximum VPD across forested areas of the northwestern U.S. for current (1980-2009) and future (2040-2069) time periods based on canopy cover and AET-to-deficit ratio. We focused on maximum VPD because of its relevance for plant growth and survival (e.g., Breshears et al. 2013, Restaino et al. 2016) and because results and patterns were very similar for maximum

temperature. Forest canopy cover was obtained from MODIS at 250 m resolution (Dimiceli 2017) and left at its native resolution for predictions. Water balance data from 1980 to 2009 at 800 m resolution (Dobrowski et al. 2013) was used to calculate the current AET-to-deficit ratio. Future projections of the AET-to-deficit ratio were calculated using climate projections for the years 2040 to 2069 with data from 20 global climate models (Table S1) that were statistically downscaled to a ~4-km spatial grain with observational data from gridMET (Abatzoglou 2013) using the Multivariate Adaptive Constructed Analogs approach (Abatzoglou and Brown 2012). We applied differences in water balance simulations from downscaled projections to baseline (1980-2009) estimates of Dobrowski et al., (2013) for compatibility between current and future predictions. Increased water use efficiency with rising carbon dioxide concentrations has been argued to buffer increases in evapotranspiration demands with increased atmospheric vapor pressure deficit and increased net radiation (Donohue et al. 2010, Swann et al. 2016). However, increased plant productivity and leaf area index with elevated CO_2 (e.g., Piao et al. 2007) may partially offset this effect. Given the uncertainty surrounding changes in ecohydrology under changing climatic conditions, we do not make adjustments in water balance calculations for rising CO_2 levels. Additionally, it is unknown how canopy cover will change over time, so we made predictions for BC under future climate conditions with present canopy cover, a 10% increase in canopy cover, and a 10% decrease in canopy cover.

Results

Daily microclimatic differences

Across all low sensors, maximum temperatures in the understory were on average 3.4°C lower than reference conditions across all levels of canopy cover, and 5.3°C lower when canopy cover was greater than 50%. Maximum VPD was on average 0.73 kPa (27%) lower in the understory across all levels of canopy cover and 1.1 kPa (38%) lower with canopy cover greater than 50%. Variation in ΔMXT and ΔVPD at the low sensors was best explained by the interaction between solar radiation and canopy cover, with a smaller effect of average wind speed (Tables S2-S4). Both ΔMXT and ΔVPD were negatively correlated with canopy cover, but the magnitude of the effect was contingent on solar radiation. Specifically, with low canopy cover, buffering of temperature and VPD decreased as solar radiation increased. In contrast, at high canopy cover, buffering of

temperature and VPD increased as solar radiation increased (Figs. 3A & C). The average ΔMXT and ΔVPD in a site with 80% canopy cover and high solar radiation (90th percentile; 310 watts/m^2) was -7.2°C and -1.7 kPa, respectively (at average wind speeds). Increased wind speed was associated with less buffering in maximum temperature and VPD between reference and understory sites. Daily differences in minimum temperature between the forest and clearing (ΔMNT) were best explained by minimum RH, average wind speed, and their interaction (Tables S2-S4). Canopy cover was not significantly related to ΔMNT; at all levels of canopy cover the minimum temperature tended to be higher in the forest than in the clearing (average ΔMNT was 3.1°C). Minimum temperature differed less between the forest and clearing when relative humidity and wind speed were high (Fig. 3B).

The differences between the understory and reference sites were less pronounced at 2 m (high) than at 10 cm (low) above the ground (Fig. 3D-F). The mean reduction in maximum temperatures at high sensors was 0.69°C across all levels of canopy cover and 1.4°C with canopy cover greater than 50%. Maximum VPD at high sensors was on average 0.24 kPa lower in the understory across all levels of canopy cover and 0.31 kPa lower with canopy cover greater than 50%. ΔMXT and ΔVPD for high sensors were best explained by soil moisture, canopy cover, and their interaction (Tables S2-S4). Both ΔMXT and ΔVPD decreased with increasing canopy cover, and at a faster rate when soil moisture was high (Fig. 3D & F; ΔMXT = -2.5°C and ΔVPD = -0.60 kPa with 80% canopy cover, 90th percentile soil moisture). There was a statistically significant relationship between canopy cover and ΔMNT for the 2-m sensors, although the marginal R^2 of the model was 0.03 and the predicted difference in minimum temperature at 80% canopy cover was small (0.61°C; Fig. 3E).

Buffering capacity

For low sensors, the 3-yr average buffering capacity (BC) for maximum temperature at each subplot was larger (indicated by more negative BC values) at sites with higher canopy cover and higher AET-to-deficit ratios ($F_{1,30}$ = 39.61, $p < 0.001$ and $F_{1,4}$ = 7.31, $p = 0.054$, respectively; Fig. 4). Although this pattern was also observed with the high sensors, it was less pronounced ($F_{1,29}$ = 30.72, $p < 0.001$ and $F_{1,4}$ = 4.96, $p = 0.087$, respectively; Fig. 4). Average BC for maximum VPD was larger (indicated by more negative BC values) at sites with high canopy cover and higher AET-to-deficit ratios, for both the low ($F_{1,31}$ = 16.11, $p < 0.001$ and $F_{1,4}$ =

17.76, p = 0.016, respectively; Fig. 4) and high sensors ($F_{1,32}$ = 15.08, p < 0.001 and $F_{1,4}$ = 9.30, p = 0.041, respectively; Fig. 4).

Under 1980-2009 conditions, most forests in the northwestern U.S. buffered maximum VPD (Fig. 5A) but this effect was limited in drier forests (e.g. eastern Oregon and central Idaho) due to low AET-to-deficit ratios and low canopy cover. Areas that strongly buffer microclimate (e.g., the wettest forests in Oregon and Washington), are predicted to lose the most buffering capacity in the future (2040-2069; Fig. 5B), although some of these forests are wetter than those of our study sites (Fig. S5). As a proportion relative to current buffering capacity (i.e., $\Delta BCP = \Delta BC/|BC_{present}|$), the eastern Cascades and forests in eastern Oregon and Washington are predicted to lose a greater proportion of their buffering capacity (Fig. 5C). Increasing future canopy cover by 10% reduced the loss of buffering capacity slightly (Figs. S6 & S7), but the majority of the landscape still lost buffering capacity due to projected changes in future climate conditions.

Discussion

Ample evidence indicates that forest canopies buffer climate extremes, but how this buffering capacity affects biotic response to warming remains poorly understood. For microclimatic buffering to ameliorate the impacts of climate change, three conditions must be met: 1) forest canopies must buffer extremes of biophysical variables that affect understory organisms, 2) buffering effects must be large enough to be biologically relevant, and 3) the effects must be temporally stable in order for them to promote the long-term persistence of understory organisms (Hylander et al. 2015). Our results suggest that forest canopies strongly buffer extremes in maximum temperature and VPD throughout the growing season, with a large enough effect to have biological implications. However, our results also highlight that microclimatic buffering is strongly dependent on water balance, which implies that the buffering capacity of forests will change over time with changes in biophysical variables, independent of changes in forest canopy cover itself.

Climate extremes can have profound consequences for biological systems and climate change is expected to increase the frequency and intensity of extreme conditions (Jentsch and Beierkuhnlein 2008, Smith 2011). Extreme maximum temperatures can affect plants directly by damaging photosynthetic apparatus (Berry and Björkman 1980) and other plant tissues (Helgerson 1990, Kolb and Robberecht 1996) or indirectly by

exacerbating drought (Adams et al. 2009, De Boeck et al. 2011, Williams et al. 2013). Plant-water relations are especially sensitive to changes in climate extremes, particularly heat waves and consequent increases in VPD that increase atmospheric demand for plant transpiration (Reyer et al. 2013). Although temperature extremes have been more frequently studied, the critical role of VPD for plant growth and survival is increasingly recognized (Breshears et al. 2013, Will et al. 2013, Restaino et al. 2016). Given the importance of microclimate and climate extremes for the distribution of understory species, tree regeneration, and primary productivity (Ohmann and Spies 1998, Geiger et al. 2003, Grimbacher et al. 2006, e.g., Arnone et al. 2008, De Boeck et al. 2011, Dingman et al. 2013), even subtle changes in microclimate and microclimate variability could alter plant species composition and carbon cycling across broad areas.

Our results clearly demonstrate that forest canopies serve to buffer microclimates, particularly near the ground surface where many organisms live. The buffering effect near the ground was as high as 16 °C and 5.0 kPa at daily time scales. On average, maximum temperatures and VPD were 5.3°C and 1.1 kPa lower, respectively, where forest canopy cover was $\geq$ 50%. While the absolute difference in maximum temperature and VPD was greater under warmer or drier conditions, proportionally (e.g., $\Delta MXT/MXT_{reference}$) the difference between the understory and the reference conditions remained fairly constant across reference maximum temperatures and VPDs. The average buffering effects that we documented are consistent with those reported in other studies (1.5°C to 5°C), spanning different vegetation types and forest structure (Suggitt et al. 2011, von Arx et al. 2013, Frey et al. 2016, Holden et al. 2016, Lenoir et al. 2017). These differences, in both temperature and VPD, are biologically significant, as experimental studies have shown that increases in temperature and/or VPD of similar magnitudes directly affect plant survival, growth, and reproduction (e.g., Will et al. 2013, Rother et al. 2015, Larson et al. 2017).

The microclimatic buffering capacity of northwestern forests will likely vary with climate change, independent of changes in canopy cover. Specifically, local water balance plays a pivotal role in determining the buffering capacity of these forests. Sites with higher moisture availability are better able to translate energy to latent as opposed to sensible heat fluxes (Dai et al. 1999) and thus provide greater microclimatic buffering. At daily timescales, microclimate buffering was most strongly related to canopy cover, consistent with other studies (von Arx et al. 2013, Frey et al. 2016, Kovacs et al. 2017), but it also varied with soil moisture, solar radiation, wind, and humidity, all components of the local water balance. Higher soil moisture was also related to greater

differences in temperature and VPD between open and forested sites in European temperate forests (von Arx et al. 2013). At the ground level, solar radiation was important because it can drive sensible heating, and under stable boundary layer conditions, this can result in large temperature differences between open areas and those under a canopy (Fridley 2009, Keppel et al. 2012). Lower wind speeds were associated with more buffering, likely due to decreased mixing. Although not measured here, forests have a frictional effect that decreases wind speeds in forested versus open areas (e.g., Raynor 1971, Chen et al. 1995), altering components of the local water balance, and further contributing to the buffering effect. Average buffering capacity across growing seasons also varied with water balance metrics. For a given level of canopy cover, subplots with higher ratios of AET to deficit had significantly greater buffering capacity. Other work has also suggested that wetter microsites are more likely to buffer temperatures at the ground level (Fridley 2009). Additionally, higher relative humidity and lower VPD have been linked to reduced temporal variability of soil and air temperatures (Ashcroft and Gollan 2013).

The role of water balance in determining forest buffering capacity has important implications for the ability of forests to act as microrefugia under changing climate conditions (De Frenne et al. 2013, Frey et al. 2016). Although we examined differences in buffering capacity across space, the strong relationship we found to water balance suggests that buffering capacity will also vary over time. The ability of forests to buffer climate extremes may diminish in areas where increased temperatures or changes in precipitation lead to decreased water availability and higher climatic water deficit, without a commensurate increase in AET. For example, sites with low AET-to-deficit ratios and open canopies, such as the eastern Cascades or lower-elevation forests in central Idaho, have minimal buffering capacity under current conditions (i.e., 1980-2009; Fig. 5A). Future predictions show that although AET will likely increase across cooler and wetter areas of the northwestern U.S., water deficits are also predicted to increase leading to a net decline in AET-to-deficit ratios (Fig. S4). Future predictions (i.e., 2040-2069) suggest large declines in buffering capacity in wetter Pacific Northwest forests. Although these forests will maintain the capacity to buffer microclimate to some extent, the microclimatic conditions in the understory are likely to become more variable as buffering capacity declines. Our projections also suggest that proportionally, the largest changes in buffering capacity will occur in low-elevation or dry forests, which currently have more limited buffering capacity. In these drier regions, microclimatic buffering by forest canopies may create important microsites in a moisture-limited system.

If forest microclimatic conditions change over time, this will have important implications for the biodiversity of northwestern forests and for the distribution of understory species. Predictions of climate change impacts on biota are increasingly incorporating microclimate and microhabitat effects (e.g., Slavich et al. 2014, Lenoir et al. 2017). While these models are improvements over those based on coarser-scale gridded data, our results suggest that these microclimates are likely to be transient. Future work should further explore the stability of microclimatic conditions and the implications of changing forest microclimates for understanding climate change impacts (Lenoir et al. 2017).

Our analyses come with three important limitations, which directly impact our ability to anticipate future changes in forest microclimates. First, the spatial scale of our analysis, ~800 m, has constraints. Within an area this large, there can be large variability in available soil moisture, due to hydrologic flow paths and plant access to groundwater. Plant communities with permanent or long-term access to groundwater (e.g., riparian areas) are likely to retain their capacity to buffer climate extremes, even as temperatures increase (McLaughlin et al. 2017, Klos et al. 2018). These local moderating effects are not captured in the analysis presented here. Furthermore, differences in incident radiation in mountainous topography, interacting with surface soil moisture result in large differences in temperature with aspect position (Holden et al. 2016) that cannot be resolved using relatively coarse data. Additionally, predictions made at the regional scale were based on canopy cover data at 250 m resolution. Within a cell this size there is variability in canopy cover that results in finer scale differences in buffering capacity. Thus our predictions should be interpreted as an average potential buffering capacity that will vary with small-scale site differences in both canopy cover and hydrology. Second, our analysis extrapolated to areas with AET-deficit-ratios outside of the range of our study sites, particularly in very wet areas. However, the AET-deficit-ratios covered by our study sites accounted for 75% and 86% of northwestern U.S. forested area under current and future conditions respectively (Fig. S5). Third, we examined three simplified potential future canopy cover scenarios; however, canopy cover will likely change in a more complex way due to human activities and direct and indirect responses to climate warming. For example, drier conditions may directly result in canopy cover declines through physiological changes in above ground to below ground plant allocations and via drought-induced forest mortality (Allen and Breshears 1998, Allen et al. 2010). Climate changes will also indirectly affect canopy cover via disturbances such as insect outbreaks and wildfires (Weed et al. 2013, Westerling 2016). Disturbances that result in complete canopy removal have the potential to cause dramatic, non-

linear changes in the microclimate conditions experienced by understory organisms. Our analysis is a first step in anticipating where forests' buffering capacity is most vulnerable to the direct impacts of climate change; however, the ultimate patterns will depend on dynamic changes in vegetation, water balance, and their interaction. Despite these uncertainties, our results suggest that current microclimates may be transient and strongly dependent on the local water balance, which in turn is expected to change with climate warming. Rapid losses in forest microclimatic buffering may amplify climate change impacts where forest canopies are lost.

Declarations

Funding – KTD, SZD, and PEH were funded by the Joint Fire Science Program (JFSP) project # 16-1-01-15. KTD and SZD were also funded by the National Science Foundation grant BCS 1461576. SZD received additional support from JFSP 15-1-03-20 and the USDA National Institute of Food and Agriculture, McIntire Stennis project [1012438]. Additional support for ZAH was provided by a NASA Applied Wildland Fire Applications award (agreement number NNH11ZDA001N-FIRES).

References

Abatzoglou, J. T. 2013. Development of gridded surface meteorological data for ecological applications and modelling. - Int. J. Climatol. 33: 121-131.

Abatzoglou, J. T. and Brown, T. J. 2012. A comparison of statistical downscaling methods suited for wildfire applications. - Int. J. Climatol. 32: 772-780.

Adams, H. D. et al. 2009. Temperature sensitivity of drought-induced tree mortality portends increased regional die-off under global-change-type drought. - Proc. Natl. Acad. Sci. USA 106: 7063-7066.

Allen, C. D. and Breshears, D. D. 1998. Drought-induced shift of a forest-woodland ecotone: Rapid landscape response to climate variation. - Proc. Natl. Acad. Sci. USA 95: 14839-14842.

Allen, C. D. et al. 2010. A global overview of drought and heat-induced tree mortality reveals emerging climate change risks for forests. - For. Ecol. Manage. 259: 660-684.

Arnone, J. A. et al. 2008. Prolonged suppression of ecosystem carbon dioxide uptake after an anomalously warm year. - Nature 455: 383-386.

Ashcroft, M. B. and Gollan, J. R. 2013. Moisture, thermal inertia, and the spatial distributions of near-surface soil and air temperatures: Understanding factors that promote microrefugia. - Agric. For. Meteorol. 176: 77-89.

Berry, J. and Björkman, O. 1980. Photosynthetic response and adaptation to temperature in higher plants. - Annu. Rev. Plant Physiol. Plant Mol. Biol. 31: 491-543.

Breshears, D. D. et al. 2013. The critical amplifying role of increasing atmospheric moisture demand on tree mortality and associated regional die-off. - Front. Plant Sci. 4: 266.

Breshears, D. D. et al. 1998. Effects of woody plants on microclimate in a semiarid woodland: Soil temperature and evaporation in canopy and intercanopy patches. - Int. J. Plant Sci. 159: 1010-1017.

Cardelús, C. L. and Chazdon, R. L. 2005. Inner-crown microenvironments of two emergent tree species in a lowland wet forest. - Biotropica 37: 238-244.

Chen, J. Q. et al. 1995. Growing-season microclimatic gradients from clearcut edges into old-growth Douglas-fir forests. - Ecol. Appl. 5: 74-86.

Chen, J. Q. et al. 1999. Microclimate in forest ecosystem and landscape ecology—variations in local climate can be used to monitor and compare the effects of different management regimes. - Bioscience 49: 288-297.

Dai, A. et al. 1999. Effects of clouds, soil moisture, precipitation, and water vapor on diurnal temperature range. - J. Clim. 12: 2451-2473.

Daly, C. et al. 2008. Physiographically sensitive mapping of climatological temperature and precipitation across the conterminous United States. - Int. J. Climatol. 28: 2031-2064.

De Boeck, H. J. et al. 2011. Whole-system responses of experimental plant communities to climate extremes imposed in different seasons. - New Phytol. 189: 806-817.

De Frenne, P. et al. 2013. Microclimate moderates plant responses to macroclimate warming. - Proc. Natl. Acad. Sci. USA 110: 18561-18565.

De Pondeca, M. et al. 2011. The Real-Time Mesoscale Analysis at NOAA's National Centers for Environmental Prediction: Current Status and Development. - Wea. Forecasting 26: 593-612.

Dimiceli, C. M. 2017. MOD44B MODIS/Terra Vegetation Continuous Fields Yearly L3 Global 250m SIN Grid V006 NASA EOSDIS Land Processes DAAC.

Dingman, J. R. et al. 2013. Cross-scale modeling of surface temperature and tree seedling establishment in mountain landscapes. - Ecol. Process. 2: 30.

Dobrowski, S. Z. 2011. A climatic basis for microrefugia: the influence of terrain on climate. - Global Change Biol. 17: 1022-1035.

Dobrowski, S. Z. et al. 2013. The climate velocity of the contiguous United States during the 20th century. - Global Change Biol. 19: 241-251.

Donohue, R. J. et al. 2010. Assessing the ability of potential evaporation formulations to capture the dynamics in evaporative demand within a changing climate. - J. Hydrol. 386: 186-197.

Frey, S. J. K. et al. 2016. Spatial models reveal the microclimatic buffering capacity of old-growth forests. - Sci. Adv. 2: e1501392.

Fridley, J. D. 2009. Downscaling climate over complex terrain: high finescale (< 1000 m) spatial variation of near-ground temperatures in a montane forested landscape (Great Smoky Mountains). - J. Appl. Meteorol. Climatol. 48: 1033-1049.

Gehlhausen, S. M. et al. 2000. Vegetation and microclimatic edge effects in two mixed-mesophytic forest fragments. - Plant Ecol. 147: 21-35.

Geiger, R. et al. 2003. The Climate Near the Ground. - Rowman and Littlefield.

Grimbacher, P. S. et al. 2006. Beetle species' responses suggest that microclimate mediates fragmentation effects in tropical Australian rainforest. - Austral Ecol. 31: 458-470.

Hannah, L. et al. 2015. Place and process in conservation planning for climate change: a reply to Keppel and Wardell-Johnson. - Trends Ecol. Evol. 30: 234-235.

Helgerson, O. T. 1990. Heat damage in tree seedlings and its prevention. - New Forests 3: 333-358.

Hietz, P. and Briones, O. 1998. Correlation between water relations and within-canopy distribution of epiphytic ferns in a Mexican cloud forest. - Oecologia 114: 305-316.

Holden, Z. A. et al. 2013. Design and evaluation of an inexpensive radiation shield for monitoring surface air temperatures. - Agric. For. Meteorol. 180: 281-286.

Holden, Z. A. et al. 2016. Development of high-resolution (250 m) historical daily gridded air temperature data using reanalysis and distributed sensor networks for the US Northern Rocky Mountains. - Int. J. Climatol. 36: 3620-3632.

Hylander, K. et al. 2015. Microrefugia: not for everyone. - Ambio 44: 60-68.

Jentsch, A. and Beierkuhnlein, C. 2008. Research frontiers in climate change: Effects of extreme meteorological events on ecosystems. - Comptes Rendus Geoscience 340: 621-628.

Keppel, G. et al. 2012. Refugia: identifying and understanding safe havens for biodiversity under climate change. - Global Ecol. Biogeogr. 21: 393-404.

Klos, P. Z. et al. 2018. Subsurface plant- accessible water in mountain ecosystems with a Mediterranean climate. - WIREs Water. e1277.

Kolb, P. F. and Robberecht, R. 1996. High temperature and drought stress effects on survival of *Pinus ponderosa* seedlings. - Tree Physiol. 16: 665-672.

Kovacs, B. et al. 2017. Stand structural drivers of microclimate in mature temperate mixed forests. - Agric. For. Meteorol. 234: 11-21.

Kuznetsova, A. et al. 2014. lmerTest: Tests for random and fixed effects for linear mixed effect models (lmer objects of lme4 package)

Larson, C. D. et al. 2017. A warmer and drier climate in the northern sagebrush biome does not promote cheatgrass invasion or change its response to fire. - Oecologia 185: 763-774.

Lenoir, J. et al. 2017. Climatic microrefugia under anthropogenic climate change: implications for species redistribution. - Ecography 40: 253–266.

Locosselli, G. M. et al. 2016. Rock outcrops reduce temperature-induced stress for tropical conifer by decoupling regional climate in the semiarid environment. - Int. J. Biometeorol. 60: 639-649.

McLaughlin, B. C. et al. 2017. Hydrologic refugia, plants, and climate change. - Global Change Biol. 23: 2941-2961.

Monteith, J. and Unsworth, M. 2008. Principles of Environmental Physics. - Academic Press.

Ohmann, J. L. and Spies, T. A. 1998. Regional gradient analysis and spatial pattern of woody plant communities of Oregon forests. - Ecol. Monogr. 68: 151-182.

Pan, Y. D. et al. 2013. The Structure, Distribution, and Biomass of the World's Forests. - Annu. Rev. Ecol., Evol. Syst. 44: 593-622.

Piao, S. L. et al. 2007. Changes in climate and land use have a larger direct impact than rising CO2 on global river runoff trends. - Proc. Natl. Acad. Sci. USA 104: 15242-15247.

Raynor, G. S. 1971. Wind and temperature structure in a coniferous forest and a contiguous field. - For. Sci. 17: 351-363.

Restaino, C. M. et al. 2016. Increased water deficit decreases Douglas fir growth throughout western US forests. - Proc. Natl. Acad. Sci. USA 113: 9557-9562.

Reyer, C. P. O. et al. 2013. A plant's perspective of extremes: terrestrial plant responses to changing climatic variability. - Global Change Biol. 19: 75-89.

Ricklefs, R. E. 1977. Environmental Heterogeneity and Plant Species Diversity: A Hypothesis. - Am. Nat. 111: 376-381.

Rother, M. T. et al. 2015. A field experiment informs expected patterns of conifer regeneration after disturbance under changing climate conditions. - Can. J. For. Res. 45: 1607-1616.

Slavich, E. et al. 2014. Topoclimate versus macroclimate: how does climate mapping methodology affect species distribution models and climate change projections? - Divers. Distrib. 20: 952-963.

Smith, M. D. 2011. The ecological role of climate extremes: current understanding and future prospects. - J. Ecol. 99: 651-655.

Stephenson, N. L. 1990. Climatic control of vegetation distribution: the role of the water balance. - Am. Nat. 135: 649-670.

Suggitt, A. J. et al. 2011. Habitat microclimates drive fine-scale variation in extreme temperatures. - Oikos 120: 1-8.

Swann, A. L. S. et al. 2016. Plant responses to increasing CO2 reduce estimates of climate impacts on drought severity. - Proc. Natl. Acad. Sci. USA 113: 10019-10024.

Varner, J. and Dearing, M. D. 2014. The Importance of Biologically Relevant Microclimates in Habitat Suitability Assessments. - PLoS ONE 9: e104648.

von Arx, G. et al. 2013. Microclimate in forests with varying leaf area index and soil moisture: potential implications for seedling establishment in a changing climate. - J. Ecol. 101: 1201-1213.

Weed, A. S. et al. 2013. Consequences of climate change for biotic disturbances in North American forests. - Ecol. Monogr. 83: 441-470.

Westerling, A. L. 2016. Increasing western US forest wildfire activity: sensitivity to changes in the timing of spring. - Philos. Trans. R. Soc. Lond., B, Biol. Sci. 371: 20150178.

Will, R. E. et al. 2013. Increased vapor pressure deficit due to higher temperature leads to greater transpiration and faster mortality during drought for tree seedlings common to the forest-grassland ecotone. - New Phytol. 200: 366-374.

Williams, A. P. et al. 2013. Temperature as a potent driver of regional forest drought stress and tree mortality. - Nat. Clim. Change 3: 292-297.

Figure Legends

Figure 1. Map of the study sites (triangles) in the northwest USA. The two sites in Oregon are too close to differentiate on the map.

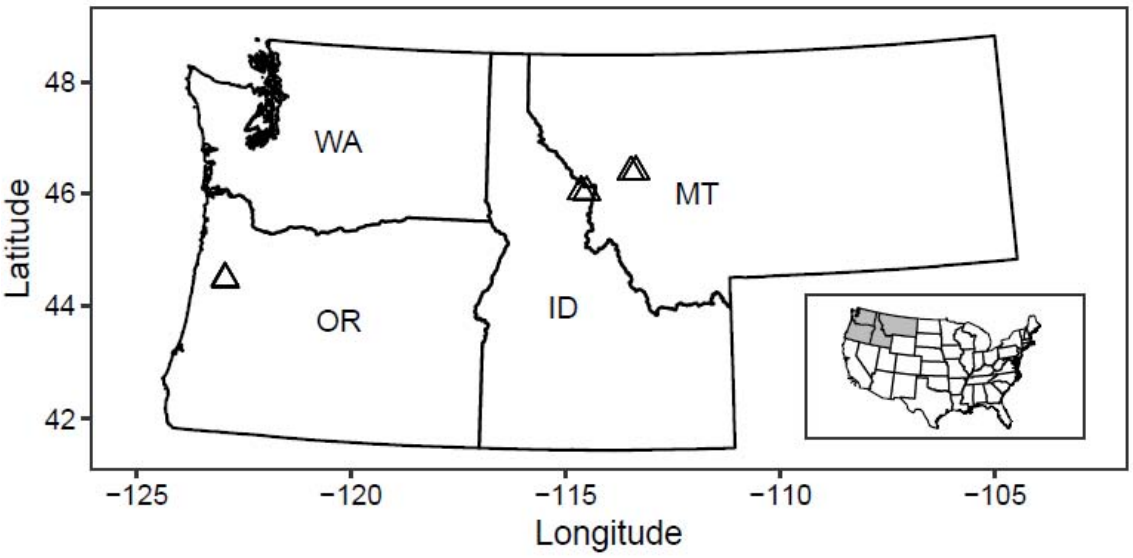

Figure 2. Examples of the relationship between maximum VPD measured under a forest canopy (understory) and maximum VPD measured out in the open at the reference sensor for two sensors at different sites. Fitted lines (solid) are derived from a linear model. The dashed line represents the 1:1 relationship. The slope of the two fitted lines are similar, however at site A the understory sensor can have either higher or lower VPD than the reference sensor depending on the reference VPD. At site B the understory sensor always has lower VPD than the reference sensor. We propose to use the area between these two lines as a measure of "buffering capacity" (BC) because it represents microclimatic buffering across the range of conditions experienced at the site. Positive values (pink) indicate overall drier conditions than at the reference site, while negative values (blue) indicate moister conditions than reference conditions.

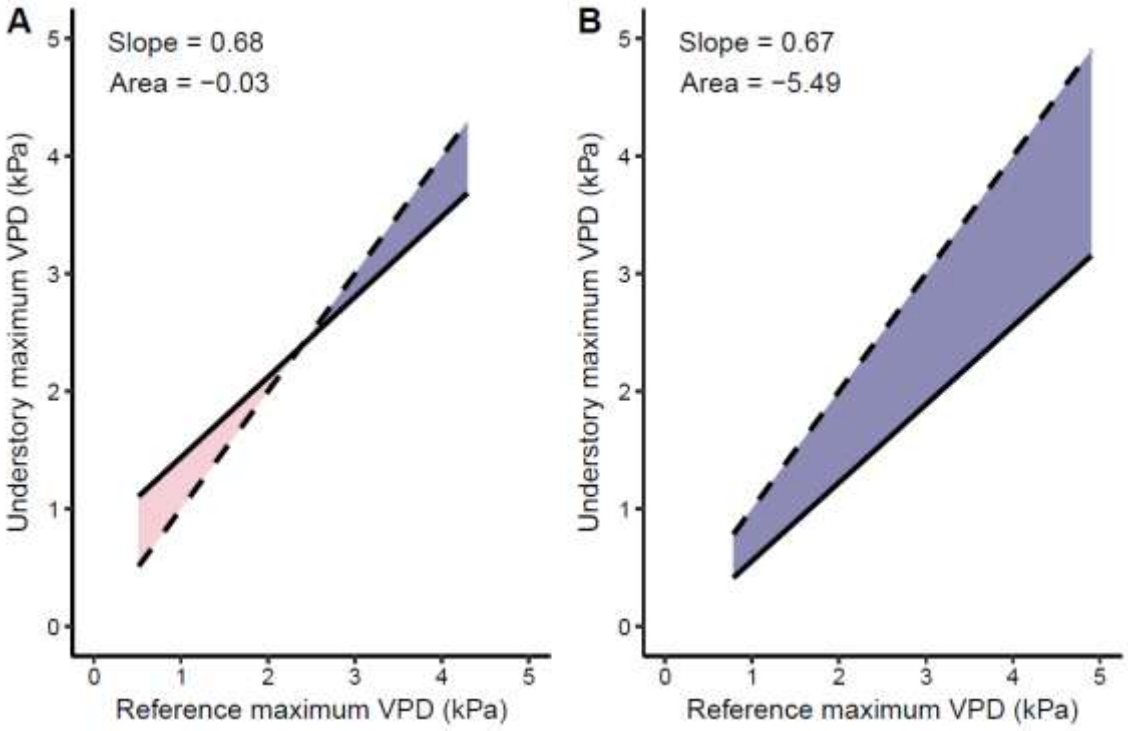

Figure 3. Fitted daily differences in maximum temperature (ΔMXT; A & D), minimum temperature (ΔMNT; B & E), and maximum VPD (ΔVPD; C & F) between understory sensors and reference sensors in the open for low (10 cm above ground; A, B, C) and high sensors (2m above ground; D, E, F) from the linear mixed effects models. Temperature differences are in degrees C and VPD differences in kPa. Results for comparisons between the ground in the forest and 2 m in the open can be found in Fig. S3.

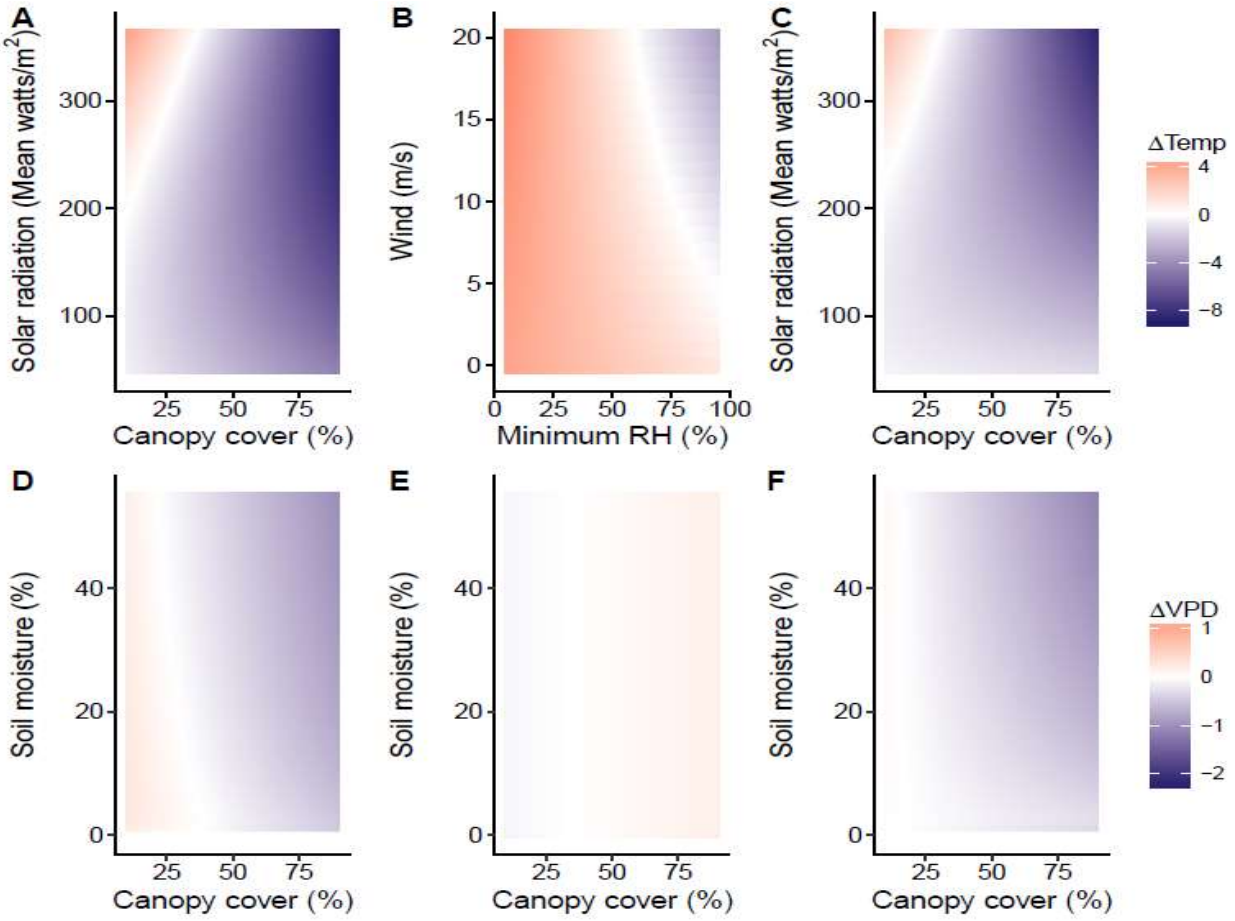

Figure 4. The buffering capacity (BC) for maximum (max) temperature and vapor pressure deficit (VPD) at high (2m above ground) and low sensors (10 cm above ground) is more negative with higher canopy cover and AET-to-deficit ratio (AET:deficit). Negative BC values indicate that it is cooler/moister in the understory than in the open.

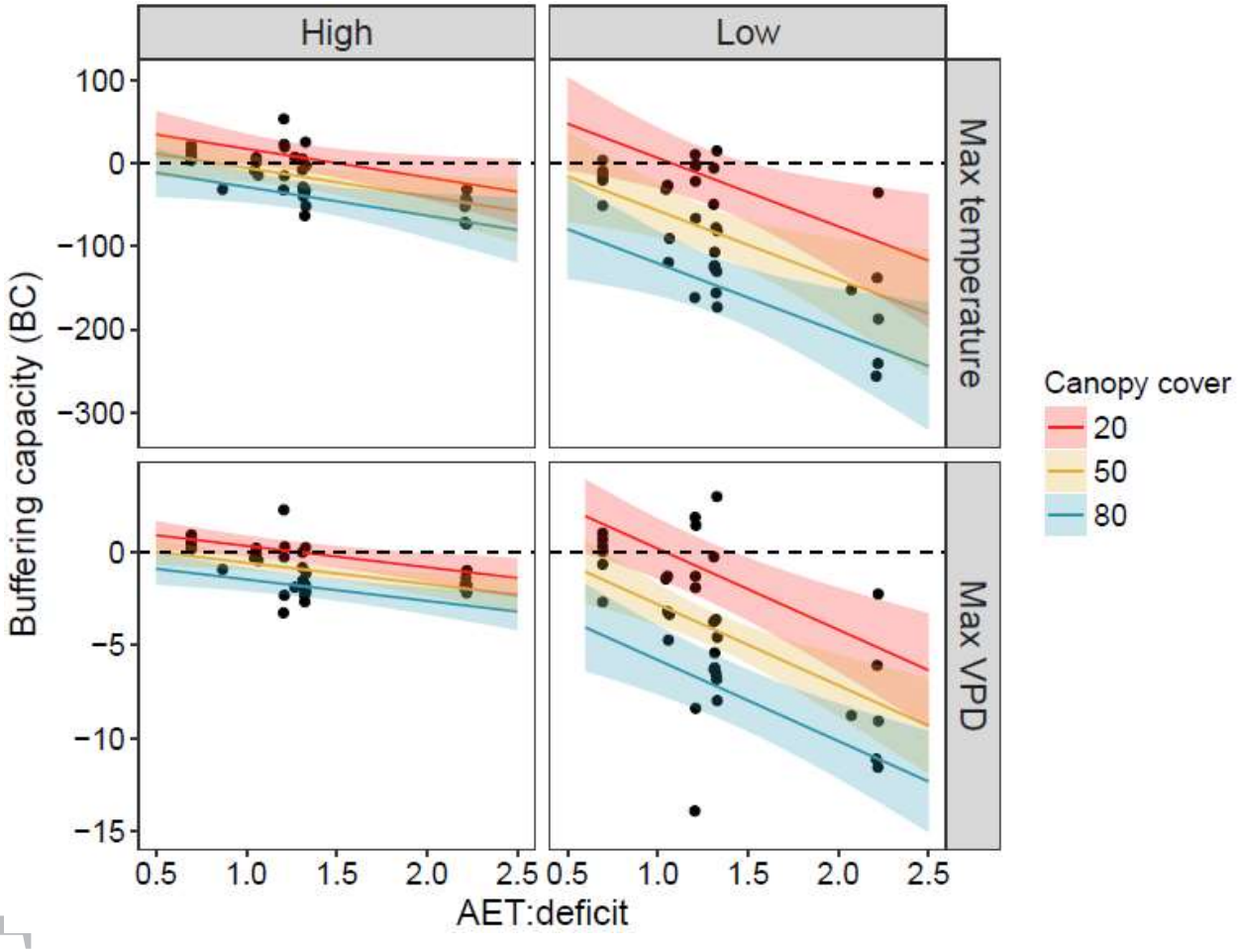

Figure 5. Microclimatic buffering capacity near the ground surface for maximum VPD under current conditions (1980-2009; A); the absolute difference between current and future (2040-2069) predicted buffering capacity (ΔBC; B); and the proportional difference between current and future predictions ($\Delta BCP = \Delta BC/|BC_{present}|$; C). Histograms to the right of plots display the distribution of cells on the landscape. Blue indicates microclimatic buffering by forests (A; moister in the understory) or a shift to greater buffering capacity in the future (B, C). Yellow indicates no difference between forest and reference conditions (A) or no change in buffering capacity over time (B, C). Red indicates it is drier in the forest (positive BC values) currently (A) or a shift towards reduced microclimatic buffering in the future (B, C). Projections are made in areas with at least 20% canopy cover which we define as forested.

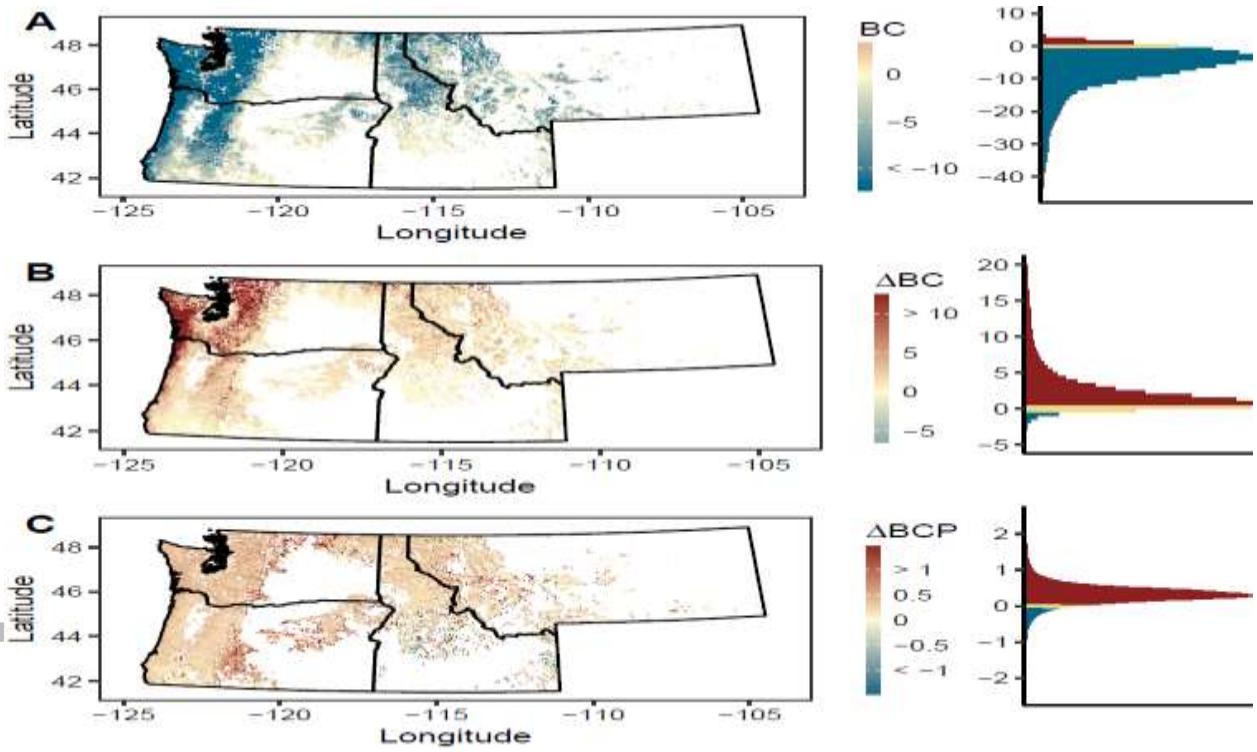

Table Legends

Table 1. Location and climate conditions of each study site. Actual annual evapotranspiration (AET) and climatic water deficit (CWD) are 30 year climate normals from 1980-2009 (Dobrowski et al., 2013). Mean maximum temperature (MXT) and mean minimum temperature (MNT) are averaged for the growing seasons 2015 and 2016 (June-September) as measured at 2 m in a clearing at each site. "Elev." is elevation.

Site	Latitude	Longitude	Elev. (m)	AET (mm)	CWD (mm)	MXT (°C)	MNT (°C)
Dunn low	44.7058	-123.316	595	504	383	27.64	12.26
Dunn high	44.6809	-123.300	1350	469	353	25.67	13.81
Clw low	46.5546	-114.683	1394	483	270	26.72	7.42
Clw high	46.5462	-114.548	1880	444	137	23.49	10.42
Lubrecht low	46.9028	-113.443	1261	378	434	27.97	7.50
Lubrecht high	46.9125	-113.323	1708	389	325	23.66	10.85